The EMBO Journal (2009) 28, 3413–3427 | © 2009 European Molecular Biology Organization | Some Rights Reserved 0261-4189/09
www.embojournal.org

THE EMBO JOURNAL

EMBO open

ATM and Artemis promote homologous recombination of radiation-induced DNA double-strand breaks in G2

Andrea Beucher[1,3], Julie Birraux[2,3], Leopoldine Tchouandong[1,3], Olivia Barton[1], Atsushi Shibata[2], Sandro Conrad[1], Aaron A Goodarzi[2], Andrea Krempler[1], Penny A Jeggo[2,*] and Markus Löbrich[1,*]

[1]Darmstadt University of Technology, Radiation Biology and DNA Repair, Darmstadt, Germany and [2]Genome Damage and Stability Centre, University of Sussex, East Sussex, UK

Homologous recombination (HR) and non-homologous end joining (NHEJ) represent distinct pathways for repairing DNA double-strand breaks (DSBs). Previous work implicated Artemis and ATM in an NHEJ-dependent process, which repairs a defined subset of radiation-induced DSBs in G1-phase. Here, we show that in G2, as in G1, NHEJ represents the major DSB-repair pathway whereas HR is only essential for repair of ~15% of X- or γ-ray-induced DSBs. In addition to requiring the known HR proteins, Brca2, Rad51 and Rad54, repair of radiation-induced DSBs by HR in G2 also involves Artemis and ATM suggesting that they promote NHEJ during G1 but HR during G2. The dependency for ATM for repair is relieved by depleting KAP-1, providing evidence that HR in G2 repairs heterochromatin-associated DSBs. Although not core HR proteins, ATM and Artemis are required for efficient formation of single-stranded DNA and Rad51 foci at radiation-induced DSBs in G2 with Artemis function requiring its endonuclease activity. We suggest that Artemis endonuclease removes lesions or secondary structures, which inhibit end resection and preclude the completion of HR or NHEJ.

The EMBO Journal (2009) **28,** 3413–3427. doi:10.1038/emboj.2009.276; Published online 24 September 2009
Subject Categories: cell cycle; genome stability & dynamics
Keywords: Artemis; ataxia telangiectasia; double-strand breaks; homologous recombination; non-homologous end joining

*Corresponding authors. PA Jeggo, Genome Damage and Stability Centre, University of Sussex, East Sussex BN1 9RQ, UK.
Tel.: +44 1273 678482; Fax: +44 1273 678121;
E-mail: p.a.jeggo@sussex.ac.uk or M Löbrich, Darmstadt University of Technology, Radiation Biology and DNA Repair, Darmstadt 64287, Germany. Tel.: +49 6151 167460; Fax: +49 6151 167462;
E-mail: lobrich@bio.tu-darmstadt.de
[3]These authors contributed equally to this work

Received: 22 June 2009; accepted: 6 August 2009; published online: 24 September 2009

Introduction

Homologous recombination (HR) and non-homologous end joining (NHEJ) represent two conceptually different pathways for repairing DNA double-strand breaks (DSBs), the lesion at the heart of many physiological and pathophysiological processes in mammalian cells. HR uses homologous sequences on the sister chromatid as a template to restore the genomic integrity upon DSB induction and involves genes of the Rad52 epistasis group (Thompson and Schild, 2002; West, 2003; Wyman and Kanaar, 2006; Thorslund and West, 2007). In contrast, NHEJ repairs DSBs without requiring sequence homology and involves the core components DNA-PKcs/Ku70/Ku80 and DNA ligase IV/XRCC4/XLF (Nussenzweig and Nussenzweig, 2007; van Gent and van der Burg, 2007). HR has a major role in repairing one-sided DSBs that arise at collapsed replication forks; it can also repair two-ended DSBs in G2-phase (Trenz *et al*, 2006; Hanada *et al*, 2007; Roseaulin *et al*, 2008). Perhaps the strongest evidence for this latter function in mammalian cells is provided by studies involving site-specific introduction of DSBs, frequently using an I-*Sce*I restriction site on plasmids or integrated model substrates (Liang *et al*, 1996; Taghian and Nickoloff, 1997; Moynahan *et al*, 1999; Johnson and Jasin, 2000; Allen *et al*, 2002). Indirect evidence for a role of HR in repairing ionizing radiation (IR)-induced DSBs is provided by the finding that HR-deficient cells exhibit increased sensitivity in the S and G2-phases of the cell cycle. However, mutants of the NHEJ pathway are exquisitely sensitive throughout the cell cycle and exhibit severe deficiency for repairing IR-induced DSBs (Rothkamm *et al*, 2003; Hinz *et al*, 2005). Here we aimed to address the role of HR in the repair of radiation-induced DSBs that arise in G2-phase.

In addition to the core components of NHEJ, several processing factors have been identified (van Gent and van der Burg, 2007; Lieber, 2008; Weterings and Chen, 2008). ATM, which is defective in the disorder, ataxia telangiectasia (A-T), and Artemis, a nuclease involved in hairpin opening during V(D)J recombination (Pannicke *et al*, 2004; Soulas-Sprauel *et al*, 2007; van der Burg *et al*, 2007), are required in non-cycling G0 cells for the repair of a subset of radiation-induced DSBs by NHEJ (Riballo *et al*, 2004; Wang *et al*, 2005; Darroudi *et al*, 2007). This subset represents the slow component of DSB repair, which are those DSBs located within or close to regions of heterochromatin (Goodarzi *et al*, 2008). Recently, we reported that ATM and Artemis also function to repair a similar sized fraction of IR-induced DSBs (approximately 15%) in G2 (Deckbar *et al*, 2007; Löbrich and Jeggo, 2007). To analyse DSB repair in G2-phase, we irradiate asynchronous cell populations with physiological doses that allow survival, and apply immunofluorescence analysis to study DSB repair by enumerating

γH2AX foci at defined times post-IR. Using centromere protein F (CENP-F) staining to identify G2 cells and aphidicolin to prevent cells in S-phase from progressing into G2 during repair incubation, we study DSBs that are generated and processed specifically in G2. We have developed a technology based on the incorporation of BrdU during repair synthesis that allows us to specifically study HR events after irradiation in G2 and also monitor the formation of RPA and Rad51 foci to assess the process of HR. Finally, we designed an approach to detect HR events based on the appearance of sister-chromatid exchanges (SCEs) that arise after IR in G2. Collectively, our findings show that NHEJ represents the major DSB-repair pathway in G2, with HR only being essential for the repair of a minor subset (~15%) of IR-induced DSBs. We show that DSB repair by HR in G2 involves ATM and Artemis endonuclease function and provide evidence that the DSBs repaired by HR are located at the heterochromatin. Thus, HR is specifically required to repair the slow DSB-repair component after exposure to X- or γ-rays. Importantly, Artemis is not a specific NHEJ factor and Artemis and ATM are involved in HR or NHEJ depending on the cell-cycle phase.

Results

DSB-repair measurements during the mammalian cell cycle

To investigate the contribution of NHEJ and HR in different cell-cycle phases, we analysed asynchronously growing cells to avoid potential introduction of DSBs during synchronization. For human fibroblasts, we used pan-nuclear CENP-F staining to identify G2 cells (Liao *et al*, 1995; Kao *et al*, 2001) and added aphidicolin to prevent irradiated S-phase cells progressing into G2 during analysis (Figure 1A). Aphidicolin caused pronounced pan-nuclear H2AX phosphorylation in S-phase cells, likely due to DSBs resulting from collapsed replication forks (Figure 1A). These S-phase cells, as well as mitotic cells, identified by their condensed chromatin and CENP-F staining were excluded from analysis. Flow cytometry (FACs) analysis demonstrated that up to 8 h post-IR the majority of irradiated G2 cells remain in G2 and that S-phase cells do not progress into G2 (Supplementary Figure 1A), providing sufficient time to detect the repair defect in ATM- and Artemis-deficient cells, which is measurable at >4 h post-IR (Riballo *et al*, 2004). To identify cell-cycle phases in mouse embryonic fibroblasts (MEFs), phosphoH3 was used instead of CENP-F (Supplementary Figure 1B). We used γH2AX foci analysis to monitor DSB repair.

Enumeration of γH2AX foci in CENP-F-positive primary human fibroblasts following 2-Gy X-irradiation provided DSB-repair kinetics in G2 (Figure 1B). Enumeration of γH2AX foci in CENP-F-negative cells, which were also negative for the pan-nuclear aphidicolin-induced γH2AX signal, allowed the analysis of repair in G1 (Figure 1B). We observed similar kinetics and magnitude of repair in G1 and G2, which was also similar to that previously observed in G0 cells (Riballo *et al*, 2004). Aphidicolin treatment did not affect the repair capacity and did not form γH2AX foci in G1 or G2 (Figure 1B). Initial γH2AX foci increased linearly with dose up to 80–90 foci per cell (Figure 1C and Supplementary Figure 1C). Foci numbers correlated with DNA content, being twice as high in G2 compared with G1 (Figure 1C). Since γH2AX foci in G1 are lost in a manner entirely dependent on NHEJ factors and represent DSBs (Riballo *et al*, 2004), the two-fold higher numbers in G2 strongly suggest that γH2AX foci in G2 also represent DSBs. To further substantiate this contention, we treated control and ATR-deficient cells with the specific ATM and DNA-PK inhibitors, KU55933 and NU7026. IR-induced γH2AX foci formation was identical between control and ATR-deficient cells and was abolished by joint KU55933/NU7026 treatment, demonstrating that ATM and DNA-PKcs, but not ATR, contribute to foci formation in G1 and G2 (Supplementary Figure 1D).

NHEJ represents the major repair pathway for IR-induced DSBs in G1 and in G2

Our previous studies utilizing CHO cells suggested that NHEJ is an important repair pathway throughout the mammalian cell cycle (Rothkamm *et al*, 2003). To substantiate this notion, we investigated mutants with deficiencies in XLF and DNA ligase IV (Lig4), two prominent NHEJ factors (Ahnesorg *et al*, 2006; Buck *et al*, 2006; Li *et al*, 2008). XLF-deficient primary human fibroblasts exhibit a pronounced repair defect in G1 and in G2, with the majority of DSBs remaining unrepaired until 8 h post-IR (Figure 2A). Similar results were obtained with Lig4-defective MEFs (Figure 2B). These observations support the model that NHEJ represents the major pathway for repairing IR-induced DSBs in G1 and in G2.

HR represents the slow component of DSB repair in G2

To examine the role played by HR in G2, we first assessed the kinetics of DSB repair in Brca2-deficient HSC62 primary human fibroblasts (Howlett *et al*, 2002). As expected, HSC62 cells show kinetics indistinguishable from those of normal human fibroblasts in G1, but, interestingly, exhibit elevated level of unrepaired DSBs at prolonged repair times (⩾4 h) in G2 (Figure 2A). Since the fast component of DSB repair (⩽2 h) is unaffected in HSC62 cells both in G1 and in G2, this suggests that HR specifically represents the slow component of DSB repair in G2, which repairs ~15% of the IR-induced DSBs. Strikingly, ATM- and Artemis-deficient cells exhibit repair kinetics indistinguishable from HSC62 cells in G2 (Figure 2A and Supplementary Figure 2). We also measured DSB-repair kinetics in MEFs deficient in ATM, Artemis or Rad54. Similar to our results with primary human fibroblasts, we observed an identical repair defect in $ATM^{-/-}$ and $Artemis^{-/-}$ MEFs affecting the slow DSB-repair component in G1 and in G2 (Figure 2B). $Rad54^{-/-}$ MEFs, in contrast, show repair kinetics indistinguishable from wild-type (WT) MEFs in G1, but a repair defect similar to ATM and Artemis in G2 (Figure 2B). Finally, we applied RNAi technology to compare deficiencies of ATM, Artemis, Brca2 or Rad51 in an isogenic background (Figure 2C). Consistent with the results using primary human fibroblasts and MEFs, HeLa cells downregulated for ATM or Artemis exhibit a repair defect in G1 and in G2, whereas cells treated with Brca2 or Rad51 siRNA show a defect only in G2, which is similar to the ATM and Artemis repair defect (Figure 2C). Significantly, the repair defects manifest only at later times (>2 h) confirming that they affect the slow component of DSB repair (Figure 2C). Collectively, these results show that HR represents the slow component of DSB repair in G2, and raise the intriguing possibility that ATM and Artemis promote HR during G2.

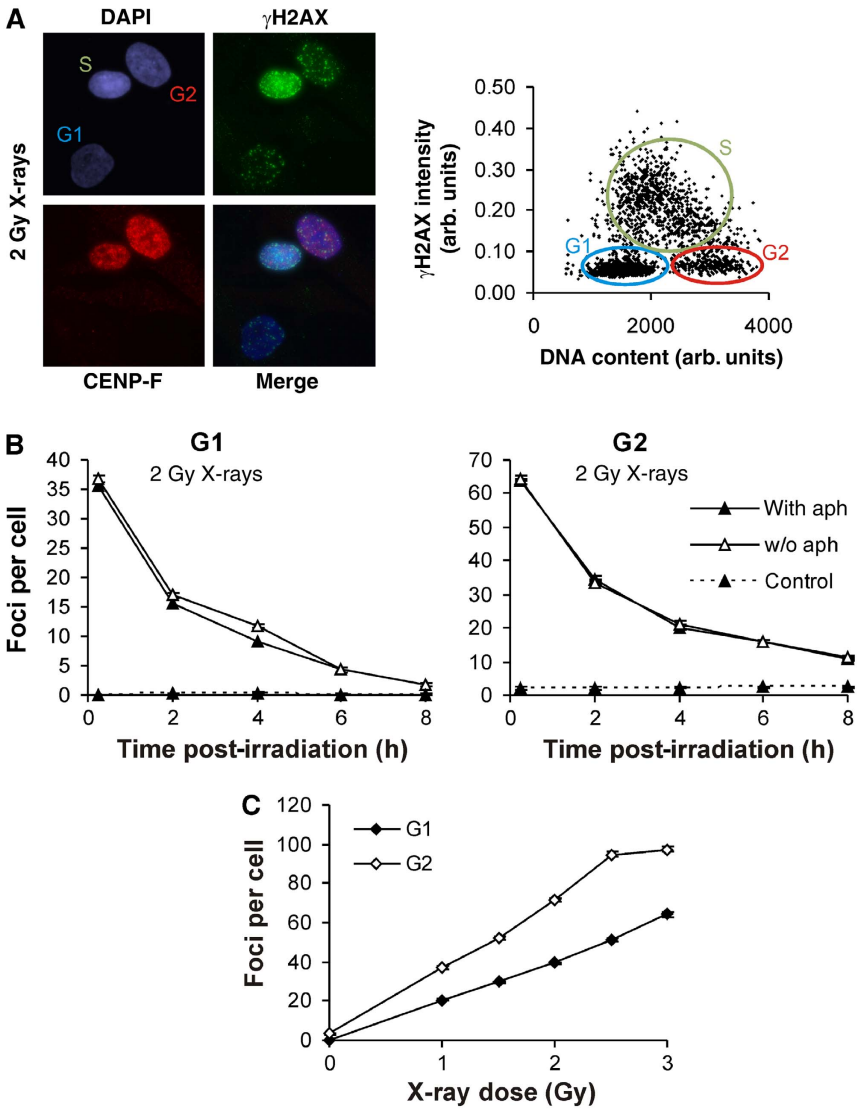

Figure 1 (**A**) Identification of cell-cycle phases in human fibroblasts (HSF1). Cells were scanned under the microscope and the γH2AX signal was plotted against the DAPI signal. S-phase cells exhibited an intermediate DAPI signal, a weak CENP-F signal and a high pan-nuclear γH2AX signal due to aphidicolin treatment. G1- and G2-phase cells were distinguished from S-phase cells by their dotted instead of a pan-nuclear γH2AX signal. G1 and G2 cells were distinguished from each other either by DAPI content (low in G1 versus high in G2) or by CENP-F staining (absent in G1 versus strong pan-nuclear in G2). Mitotic cells exhibited CENP-F staining and condensed chromatin (Deckbar *et al*, 2007), and were excluded from the analysis. (**B**) DSB repair in G1- and G2-phase HSF1 cells is unaffected by aphidicolin treatment and aphidicolin itself (designated 'control' in the figure) does not induce γH2AX foci. (**C**) γH2AX foci formation in HSF1 cells at 15 min post IR is linear with dose in G1 and G2 up to approximately 80 foci per cell. G2 cells exhibit about twice the number of DSBs as G1 cells, consistent with their two-fold higher DNA content (NB: The number of DSBs observed in G2 phase at later times (e.g. 8 h) is routinely higher than twice the number in G1-phase since the slow component of DSB repair in G2 is slower than in G1). Error bars in panels B and C represent the s.e.m. from analysis of at least 40 cells.

Artemis- and ATM-deficient cells show a defect in IR-induced repair synthesis during HR in G2

Since HR repairs only ~15% of the IR-induced DSBs in G2, and since γH2AX foci loss monitors all repair events, that is, NHEJ and HR, we sought alternative techniques, which would more specifically measure HR of IR-induced DSBs in G2. We developed a technique, which is based on microscopic detection of BrdU that is incorporated into DNA during repair by HR when extensive DNA regions are synthesized (Figure 3). In this assay, BrdU is added during repair, that is, after irradiation, and the DNA is denatured for analysis. Aphidicolin was added and CENP-F was used to discriminate between G1, S and G2 cells, similar to our cell-cycle-specific approach for measuring γH2AX foci. Distinct BrdU foci after irradiation were observed only in G2 cells exhibiting pronounced CENP-F staining and high (4N) DNA content. S-phase cells with faint CENP-F staining and intermediate DNA content showed pronounced pan-nuclear BrdU signal and were excluded from analysis. The pronounced BrdU signal of S-phase cells in the presence of aphidicolin is consistent with the pronounced pan-nuclear γH2AX signal of these cells (Figure 1A), and may suggest that DSBs arising due to aphidicolin treatment are repaired by HR. Importantly, G1 cells negative for CENP-F and exhibiting low DNA content did not show any BrdU incorporation, demonstrating that any DNA synthesis during NHEJ is undetectable by this technique (Figure 3). The number of HR sites monitored with this assay in G2 cells increases with repair time and inversely correlates

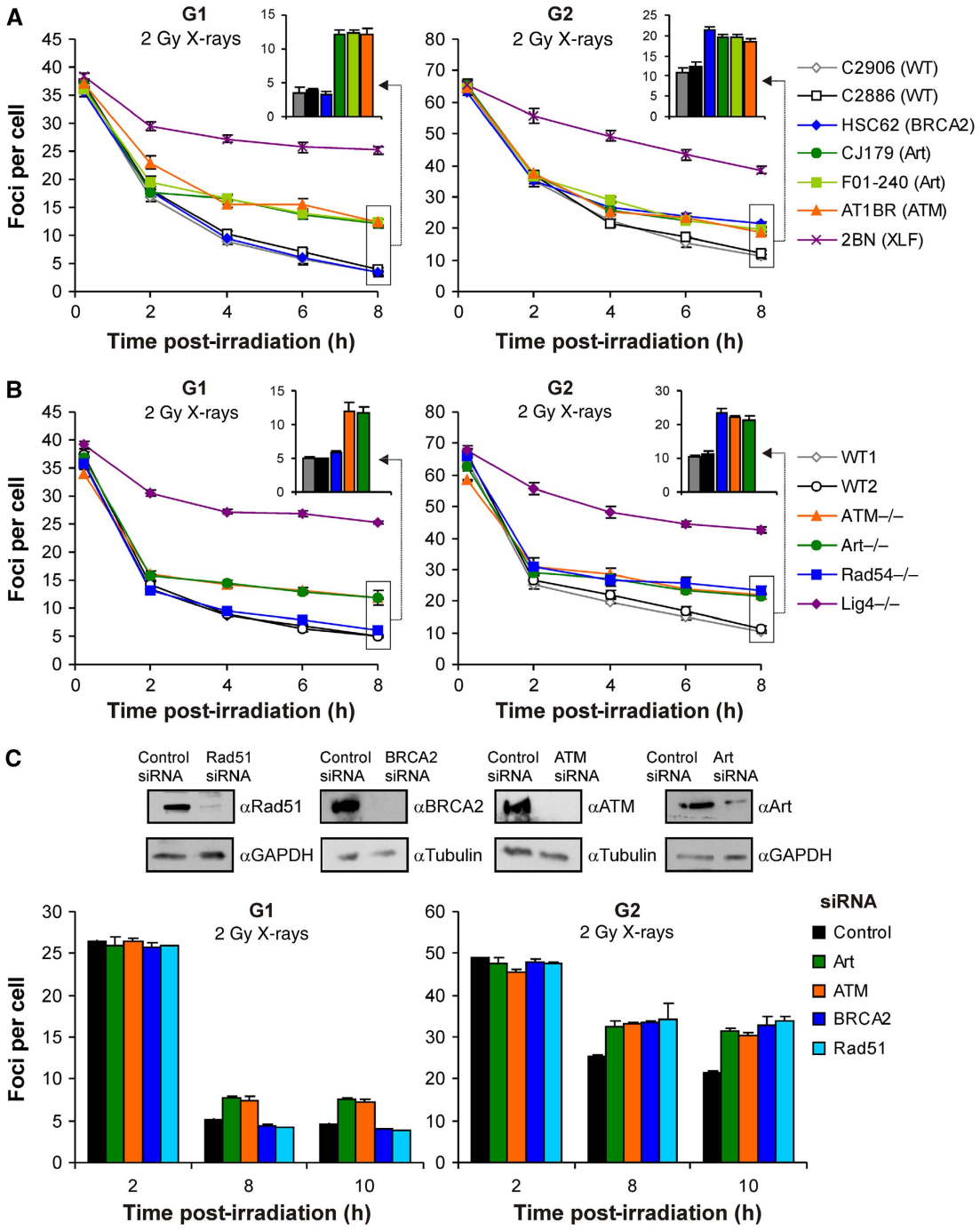

Figure 2 (**A**) γH2AX foci analysis in primary human fibroblasts. Background foci numbers in primary human fibroblasts were about 2 in G2 and 0.2 in G1, and were subtracted from the foci numbers in the irradiated samples. (**B**) γH2AX foci analysis in MEFs. Background foci numbers in MEFs were about 2–4 in G2 and 0.5–2 in G1, and were subtracted from the foci numbers in the irradiated samples. The insets magnify the 8-h data for WT, Brca2-; Rad54-, Artemis- and ATM-deficient cells. Statistical analysis was performed at the 6- and 8-h time points, and revealed that Artemis- and ATM-deficient cells in G1 and G2, and Brca2- and Rad54-deficient cells in G2 exhibit significantly elevated foci levels compared with WT cells ($P<0.05$; one-tailed Welch's test). (**C**) γH2AX foci analysis in siRNA-treated HeLa cells analysed 48 h after transfection. Efficient knockdown to protein levels <20% was confirmed for all tested siRNAs by Western blotting. Background foci numbers in HeLa cells were about 2–4 in G2 and 0.5–2 in G1, and were subtracted from the foci numbers in the irradiated samples. The number of induced foci measured at 15 min post-IR was similar for all siRNA conditions (data not shown). Samples were evaluated in a blinded manner. Statistical analysis was performed and revealed that cells depleted for Artemis or ATM in G1 and G2, and for Brca2 and Rad51 in G2 exhibit significantly elevated foci levels compared with control siRNA-treated cells at the 8- and 10-h time points ($P<0.05$; one-tailed Welch's test). Although the repair defect is apparent and similar for the different cell systems, the absolute foci numbers in HeLa cells are higher, likely due to their higher DNA content. Error bars in panels A–C represent the s.e.m. from at least three different experiments.

with the slow component of loss of γH2AX foci (HeLa cells depleted for Brca2 or Rad51 exhibit ~7 more γH2AX foci than control cells at 8 h following 2-Gy irradiation treatment, while the BrdU incorporation assay monitors ~14 BrdU sites at 8 h following 4-Gy irradiation treatment; compare Figure 3 with Figure 2C). The specificity of the assay is further shown by its

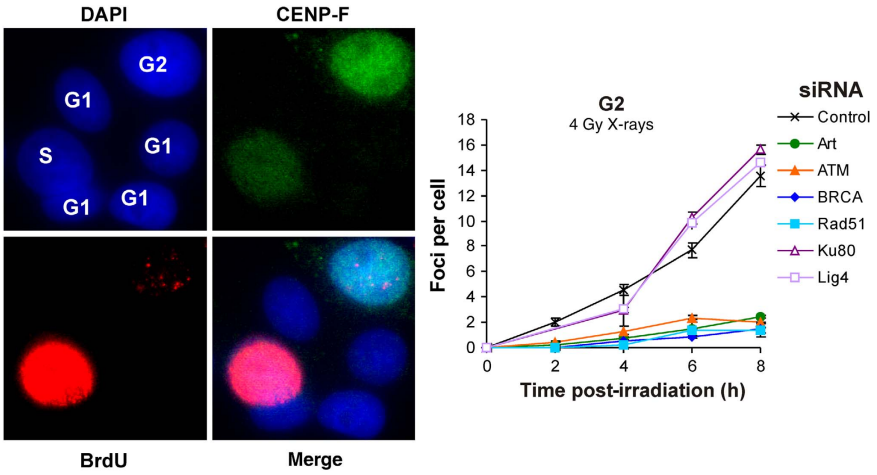

Figure 3 HR repair sites were visualized by incorporation of BrdU during repair synthesis. HeLa cells were irradiated with 4 Gy and BrdU was added for the entire repair time—BrdU foci were observed after denaturing conditions in G2- but not in G1-phase cells. S-phase cells were identified by pan-nuclear γH2AX or BrdU staining and excluded from the analysis. The image on the left shows control cells analysed 8 h following 4-Gy irradiation treatment. Efficient knockdown to protein levels <25% was confirmed by Western blotting and γH2AX foci analysis (Supplementary Figure 3). Error bars represent the s.e.m. from the analysis of three different experiments (two experiments for Ku80 and Lig4 siRNA).

strict requirement for Rad51 and Brca2. Moreover, depletion of Ku80 or Lig4 does not substantially affect BrdU foci levels (Figure 3 and Supplementary Figure 3). Significantly, Artemis and ATM depletion leads to complete lack of HR sites, providing strong evidence that Artemis and ATM promote HR of IR-induced DSBs in G2 (Figure 3).

ATM and Artemis are required for IR-induced SCEs in G2

We sought further evidence for a role of ATM and Artemis in promoting G2 HR and studied the formation of SCEs as a well-established marker for HR events (Sonoda *et al*, 1999 and Figure 4). We grew HeLa cells in BrdU-containing medium for two cell cycles, added aphidicolin immediately before irradiation with 2 Gy to exclude the S-phase cells from analysis and collected metaphases up to 12 h post-IR. Pilot experiments had shown that G2 cells irradiated with 2 Gy enter mitosis between 8 and 12 h after irradiation (data not shown and Deckbar *et al*, 2007). Hence, this procedure monitors SCE formation arising from HR in G2-phase. We observed ~7 SCEs per cell in un-irradiated cells, which increased to ~14 SCEs per cell after IR treatment (Figure 4). Downregulation of Rad51 or Brca2 by siRNA led to significant reduction in the spontaneous SCE level and completely abolished the formation of radiation-induced SCEs (Figure 4). Spontaneous SCEs are likely produced during the preceding cell cycles when siRNA downregulation is ongoing but not yet optimal. Thus, the reduction observed after Rad51 or Brca2 depletion probably represents an underestimation. In contrast to the effects of Rad51 and Brca2, neither spontaneous nor IR-induced SCE level is significantly affected by depleting Ku80 or Lig4. Most importantly, downregulation of Artemis or ATM does not substantially affect the spontaneous SCE level, but nearly completely abolishes the increase observed after irradiation (Figure 4). Hence, Artemis and ATM play a major role in promoting HR of IR-induced DSBs in G2, but are unlikely to represent core components of the HR machinery.

We also examined whether Artemis and ATM are involved in HR using a plasmid-based I-*Sce*I system (Supplementary Figure 4). We measured the frequency of reconstitution of a GFP reporter gene within a chromosomally integrated plasmid substrate in transformed human fibroblasts with or without silencing of Artemis, ATR or Brca2 (Supplementary Figure 4A), as previously described (Pierce *et al*, 1999). Transient expression of the I-*Sce*I endonuclease generates a DSB, which can be repaired by gene conversion, yielding a functional GFP gene whose expression can be assessed by flow cytometry (Supplementary Figure 4B). Consistent with previous studies (Moynahan *et al*, 2001; Wang *et al*, 2004), we observed significant reduction in I-*Sce*I-induced HR after depletion of Brca2 or ATR, but failed to observe any effect in cells depleted for Artemis (Supplementary Figure 4C). Moreover, there was only a small impact (approximately one-third) caused by inhibiting ATM (Supplementary Figure 4C). The ATR dependency perhaps suggests that this assay preferentially monitors HR events occurring during S-phase. In any case, the lack of a pronounced dependency on ATM or Artemis confirms that these factors are not core HR enzymatic components.

RPA, Rad51 and ssDNA foci formation is compromised in ATM- and Artemis-deficient cells

Our approaches using quantification of BrdU incorporation during HR, as well as assessment of SCE levels in G2-irradiated cells, provided strong evidence that ATM and Artemis are defective in a pathway of HR. To examine at which point the proteins might act and to gain further evidence for impaired HR, we examined the intermediates in the reaction (Figure 5). RPA and Rad51 form IR-induced foci, which have been suggested to represent sites of resected DSBs (Miyazaki *et al*, 2004; Bekker-Jensen *et al*, 2006; Sartori *et al*, 2007). Consistent with this, we observed that Rad51 foci are restricted to S- and G2-phase cells, and examined foci specifically in G2 cells. RPA and Rad51 foci in G2 form linearly with dose up to ~6 Gy (Supplementary Figure 5A–C). Time-course analysis revealed that the maximum number is formed at 2–3 h post-IR, which then decreases. The rate of decrease parallels the slow component

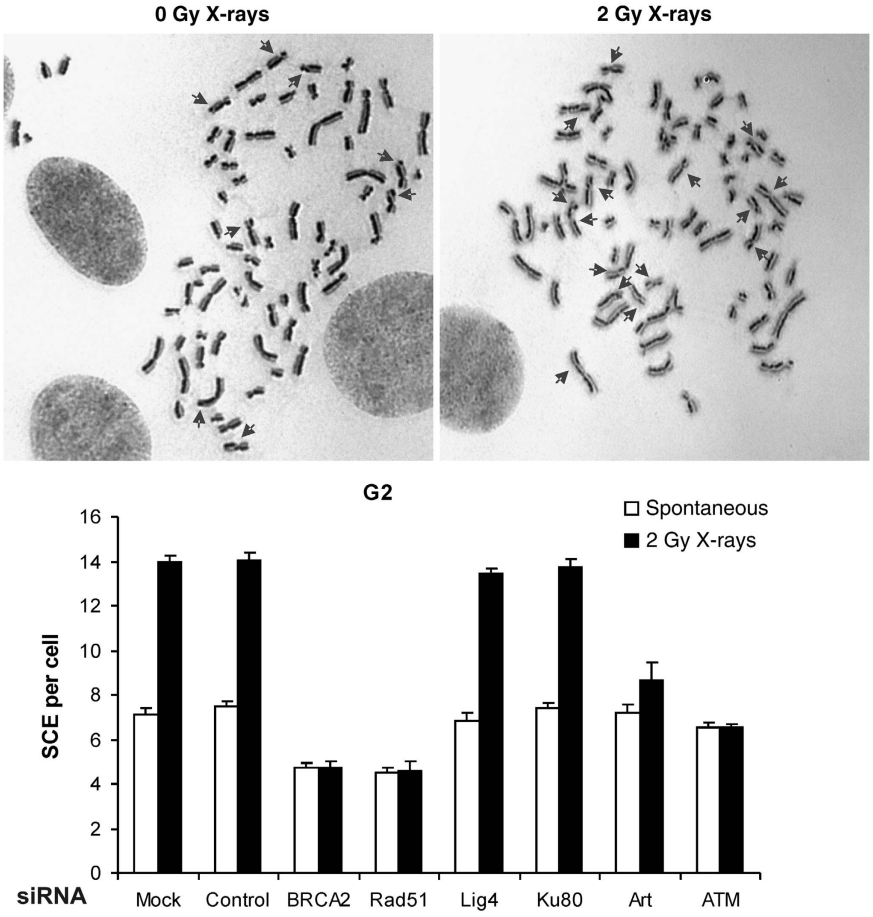

Figure 4 SCEs are detected in G2-irradiated HeLa cells. Cells were grown for two cell cycles (48 h) in BrdU-containing medium and aphidicolin was added immediately prior to irradiation with 2 Gy. Colcemid was then added at 8 h post-IR and the samples were harvested at 12 h post-IR. Irradiation was performed 48 h after siRNA transfection. Samples designated 'mock' were treated with transfection reagents, but no siRNA was added. SCE numbers were normalized to 70 chromosomes to account for the variability in chromosome number between metaphases. At least 100 metaphases from at least three different experiments were analysed. Error bars represent the s.e.m. from all analysed metaphases.

of DSB repair. The maximum number of 15–20 foci observed after a dose of 2 Gy is consistent with our notion that approximately 15–20% of the IR-induced DSBs are repaired by HR in G2 (based on an induction rate of 50 DSBs per Gy per G2 cell; Kegel *et al*, 2007), and our finding that NHEJ repairs the majority of DSBs in G1 and G2.

RPA and Rad51 foci formation is significantly compromised in primary human A-T fibroblasts (Figure 5A), consistent with previous observations (Morrison *et al*, 2000; Yuan *et al*, 2003; Shrivastav *et al*, 2009). Strikingly, Artemis-deficient fibroblasts show a defect in RPA and Rad51 foci formation similar to that of A-T cells (Figure 5A), substantiating our conclusion that Artemis and ATM promote HR in G2. We also investigated Brca2-deficient fibroblasts and observed, in contrast to ATM- and Artemis-deficient cells, normal formation of RPA foci. However, RPA foci failed to disappear with time in Brca2-deficient cells, remaining at ~20 foci per cell (after 2 Gy IR) for up to 8 h (Figure 5A). At this time, the level of RPA foci is similar to that of γH2AX foci (see Figure 2A), suggesting that all unrepaired DSBs in Brca2-deficient cells exhibit unresolved RPA foci. Consistent with the requirement of Brca2 for Rad51 foci formation (Yuan *et al*, 1999; Esashi *et al*, 2007), we failed to observe Rad51 foci in Brca2-deficient cells. Moreover, HeLa cells downregulated for CtIP, a newly identified protein that promotes end resection during HR (Sartori *et al*, 2007; Huertas *et al*, 2008), show a severe defect in Rad51 and RPA foci formation (Figure 5B and data not shown).

Finally, we developed a BrdU staining technique to detect the presence of single-stranded DNA (ssDNA) intermediates in G2-phase cells, which we considered would be representative of HR rather than NHEJ (Figure 5C). In this assay, cells are prelabelled with BrdU for 24 h and BrdU foci are detected under non-denaturing conditions. Importantly, this assay directly measures the presence of ssDNA without relying on the detection of recruited or modified repair factors (such as RPA or Rad51). We observed BrdU foci in G2- but not in G1-phase cells, which increase up to 2 h and then decrease with kinetics similar to the loss of RPA or Rad51 foci. We observed persistent ssDNA intermediates in Rad51-depleted cells, consistent with the notion that ssDNA arises but HR does not proceed without Rad51. Strikingly, HeLa cells downregulated for ATM or Artemis show substantially reduced ssDNA formation, verifying their role in promoting end resection during IR-induced HR in G2 (Figure 5C).

Taken together, the formation and loss of RPA and Rad51 foci correlates with the subset of DSBs that is repaired by HR. Moreover, Rad51 foci do not form in cells lacking Brca2, CtIP or Rad51, substantiating the specificity of the assay. Strikingly, RPA and Rad51 foci, as well as formation of

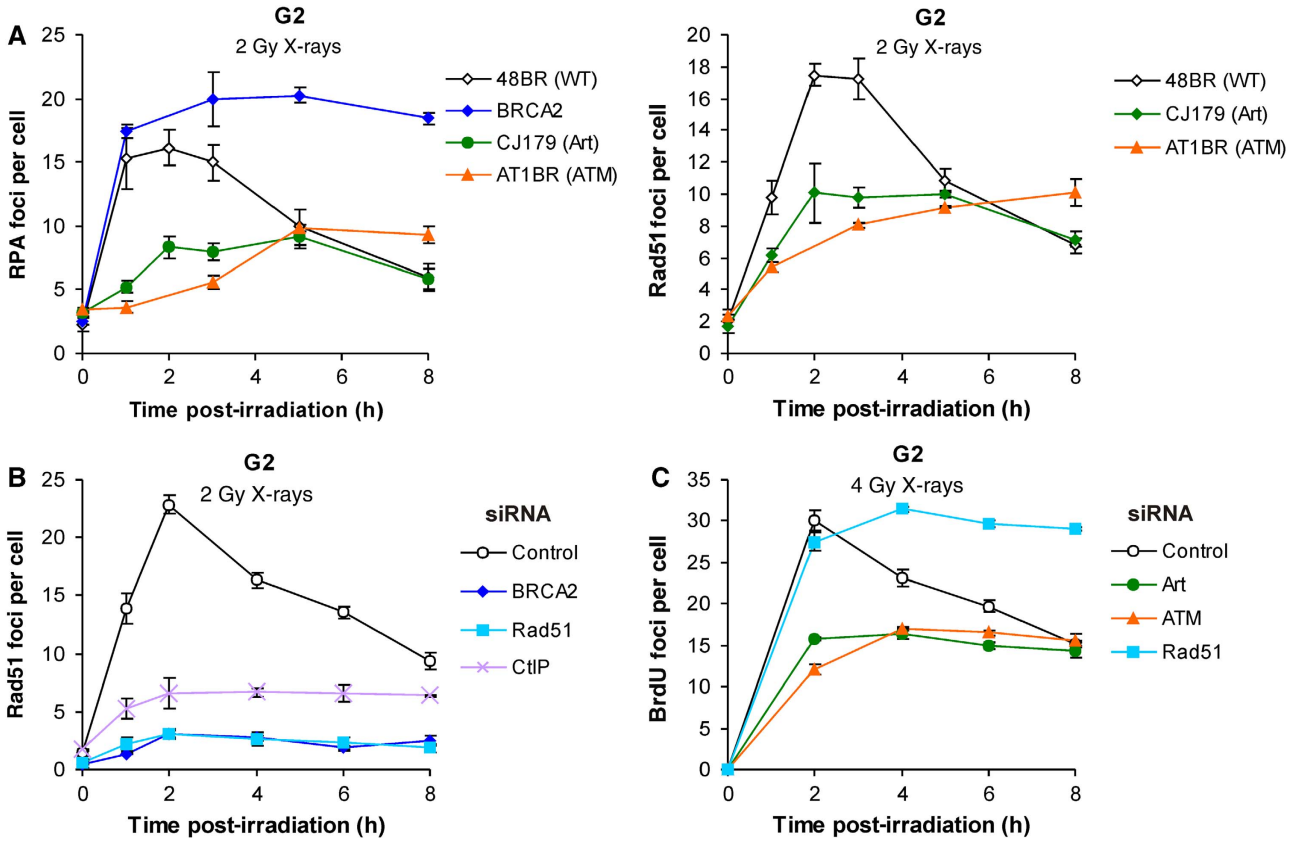

Figure 5 ssDNA formation is compromised in ATM/Artemis-deficient cells. (**A**) Analysis of RPA and Rad51 foci formation in primary human fibroblasts. (**B**) Analysis of Rad51 foci formation in siRNA-treated HeLa cells. (**C**) Analysis of ssDNA by measuring BrdU foci in siRNA-treated HeLa cells. Cells were labelled with BrdU for 24 h prior to irradiation and foci were observed after non-denaturing conditions. Error bars represent the s.e.m. from the analysis of at least three different experiments.

ssDNA, are considerably reduced in ATM- and Artemis-deficient cells.

Epistasis analysis confirms that ATM and Artemis function in the same pathway as Brca2, Rad51 and Rad54 for repairing radiation-induced DSBs in G2

We next wished to confirm our finding that ATM and Artemis promote HR in G2 by γH2AX foci counting in combination with epistasis analysis. Addition of the ATM inhibitor, KU55933, to WT, Artemis- and Brca2-deficient cells confirmed that ATM and Artemis function in the same repair pathway in G1 and G2, which is epistatic with Brca2 in G2 (Figure 6A). Importantly, KU55933 increased the level of unrepaired DSBs in XLF-deficient primary human fibroblasts in G2 but not in G1 (Figure 6A). Indeed, the elevation in the level of unrepaired DSBs conferred by KU55933 in G2 appears to be the same in XLF-deficient cells and in WT cells. Hence, in G2, there is additivity for the loss of XLF and ATM instead of epistasis. Further, KU55933 did not affect foci levels in Rad54$^{-/-}$ MEFs in G2, demonstrating epistasis between ATM and Rad54 in G2 (Figure 6B). In contrast, KU55933 increased foci levels in Lig4$^{-/-}$ MEFs in G2 (Figure 6B). XRCC2$^{-/-}$ MEFs provided results similar to Rad54$^{-/-}$ MEFs (Supplementary Figure 6). We also applied RNAi technology to exclude the possibility that KU55933 has off-target effects (Figure 6C). HeLa cells downregulated in the combinations ATM/Brca2, ATM/Rad51, Artemis/Brca2 or Artemis/Rad51 show a defect similar to that observed after downregulation of the individual factors (Figure 6C). Taken together, this confirms our finding that ATM and Artemis function in the same pathway as Brca2, Rad51 and Rad54 for repairing radiation-induced DSBs in G2.

As an alternative approach to examine DSB repair in primary human fibroblasts, we induced premature chromosome condensation (PCC) in G2-phase cells using the phosphatase inhibitor calyculin A. G2 cells are readily distinguished from mitotic cells and allow analysis of PCC breaks (Asakawa and Gotoh, 1997). Enumeration of PCC breaks in G2-phase chromosomes confirmed a repair defect in Artemis- and Brca2-deficient cells at 4 and 6 h, which is not observable at 1 h following 1-Gy IR treatment, a phenotype consistent with the analysis of γH2AX foci (Figure 6D). ATM inhibition in WT, Artemis- and Brca2-deficient cells confirmed that ATM, Artemis and Brca2 operate in the same pathway of DSB repair in G2 (Figure 6D).

Taken together, our epistasis studies applying γH2AX foci analysis and PCC technology show that ATM and Artemis function in the same DSB repair pathway as Brca2, Rad51 and Rad54 in G2, and, hence, confirm the notion that ATM and Artemis have a role in promoting HR of IR-induced DSBs in G2.

Artemis-dependent DSB repair in G2 does not require DNA-PK activity

Artemis' role in V(D)J recombination and IR-induced DSB repair in G1 has been shown to require DNA-PK activity (Riballo *et al*, 2004; Goodarzi *et al*, 2006; van Gent and van

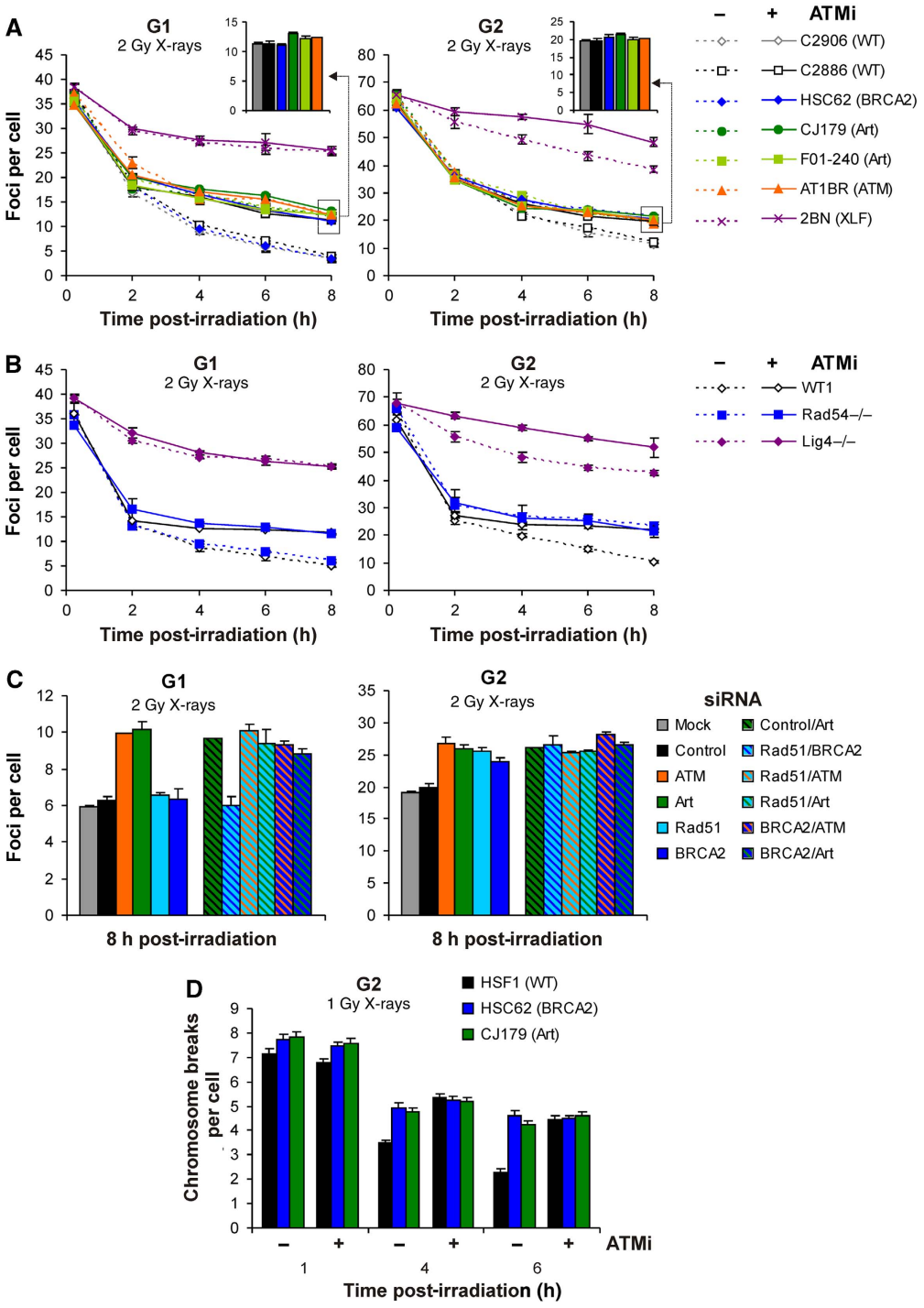

Figure 6 (**A**) γH2AX foci in primary human fibroblasts in the presence or absence of the ATM inhibitor, KU55933 (designated ATMi in the figure). The insets magnify the 8-h data for WT, Brca2-; Artemis- and ATM-deficient cells treated with KU55933. (**B**) γH2AX foci analysis in MEFs in the presence or absence of KU55933. Statistical analysis was performed at the 6- and 8-h time points, and revealed that XLF- and Lig4-deficient cells treated with KU55933 exhibit significantly elevated foci levels compared with untreated XLF- and Lig4-deficient cells in G2 but not in G1 ($P<0.05$; one-tailed Welch's test). (**C**) γH2AX foci analysis in siRNA-treated HeLa cells. Samples were evaluated in a blinded manner. Statistical analysis was performed and revealed that cells depleted for Artemis, ATM, Control/Artemis, Rad51/Artemis, Rad51/ATM, Brca2/Artemis and Brca2/ATM in G1 and G2, and Rad51-, Brca2- and Rad51/Brca2-depleted cells in G2 exhibit significantly elevated foci levels compared with control siRNA- and mock-treated cells ($P<0.05$; one-tailed Welch's test). Samples designated 'mock' were treated with transfection reagents, but no siRNA was added. The experiments for panels A–C were carried out as for Figure 2. Error bars represent the s.e.m. from at least three different experiments. (**D**) Analysis of G2 PCC chromosomal breaks in calyculin A-treated primary human fibroblasts in the presence of aphidicolin and in the presence or absence of KU55933. Breaks in un-irradiated samples were less than 0.2 and were subtracted from the breaks in the irradiated samples. Error bars represent the s.e.m. from at least 100 cells. Statistical analysis revealed that Brca2- and Artemis-deficient cells with and without KU55933 exhibit significantly more PCC breaks than WT cells without KU55933 at 4 and 6 h ($P<0.05$; one-tailed Welch's test).

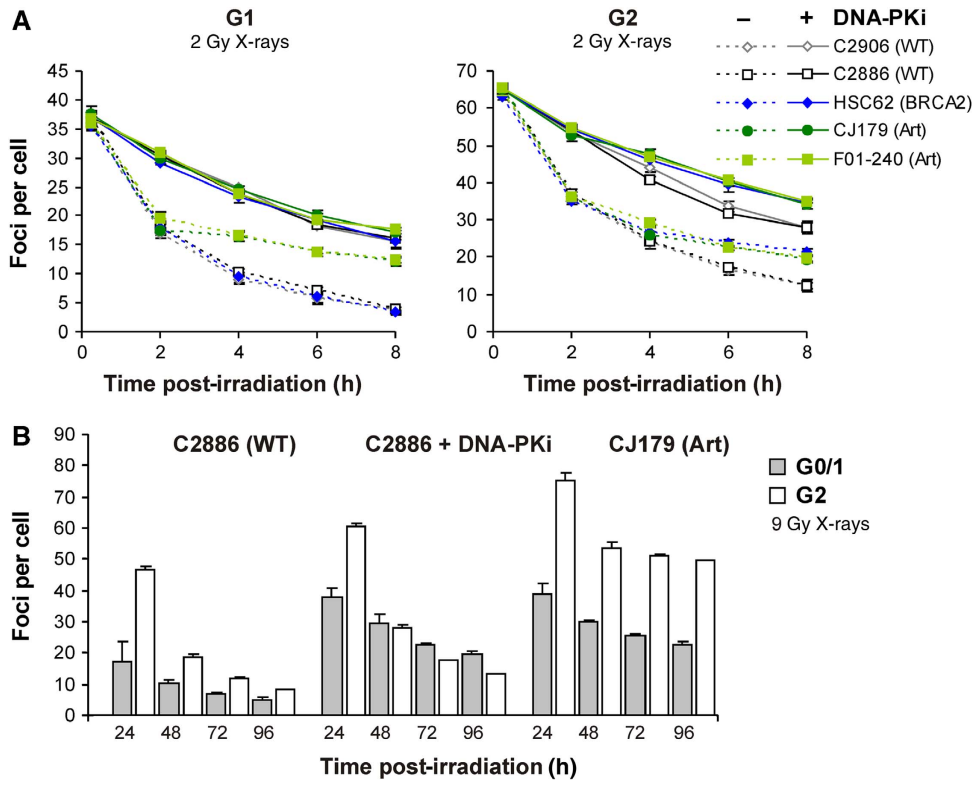

Figure 7 (**A**) γH2AX foci analysis in primary human fibroblasts in the presence or absence of the DNA-PK inhibitor, NU7026 (designated DNA-PKi in the figure). The analysis was carried out as for Figure 2A. Statistical analysis was performed at the 6- and 8-h time points, and revealed that Artemis- and Brca2-deficient cells with NU7026 exhibit significantly elevated foci levels compared with WT cells with NU7026 in G2 but not in G1 ($P<0.05$; one-tailed Welch's test). (**B**) γH2AX foci analysis at prolonged times after IR. Using an approach, which circumvents aphidicolin treatment, cells were pulse-labelled with BrdU for 1 h and irradiated with 9 Gy 4 h after labelling (when in G2). Due to the higher dose, the majority of irradiated G2 cells remained in G2 for at least 96 h (Supplementary Figure 7A). Foci were analysed in BrdU-positive cells and taken to represent G2 cells. The few BrdU-positive cells that had progressed from G2 into G1 during repair incubation were excluded from the analysis based on their lower DAPI signal compared with that of G2 cells. Data for G0 cells were obtained in parallel experiments from the analysis of confluent cultures. Results similar to G0 were obtained for G1 from the analysis of BrdU-negative cells (representing mainly G1 cells) in the same samples that were analysed for the G2 data (Supplementary Figure 7B). The continuing activity of NU7026 over 96 h was confirmed in control experiments (Supplementary Figure 7C). Error bars represent the s.e.m. from the analysis of at least three different experiments.

der Burg, 2007). Given its involvement in HR and the finding that it functions independently of XLF and Lig4 in G2, we next tested whether Artemis functions in G2 independently of DNA-PK activity. Treatment of WT primary human fibroblasts with the DNA-PK inhibitor, NU7026, resulted in substantially impaired DSB-repair kinetics in both G1 and G2, consistent with evidence that NHEJ has a major role in both cell-cycle phases. In G1, NU7026-treated, Artemis-deficient cells exhibit the same defect as NU7026-treated WT cells (Figure 7A). Thus, loss of Artemis does not confer an additional repair defect in a DNA-PK-deficient background, consistent with Artemis' role requiring DNA-PK (Riballo *et al*, 2004). However, in G2, NU7026-treated, Artemis-deficient cells show a repair defect greater than that observed in NU7026-treated WT cells (Figure 7A). Indeed, the elevation in the level of unrepaired DSBs in DNA-PKcs-inhibited, Artemis-deficient cells (relative to WT cells) appears to be the sum of the elevation in DSBs in cells deficient for Artemis and in cells inhibited for DNA-PKcs. Hence, in G2, there is additivity for the loss of Artemis and DNA-PKcs instead of epistasis.

We have previously shown that Artemis-independent DSBs in G1 can be repaired without DNA-PKcs, although at a reduced rate, and that the level of unrepaired DSBs in a DNA-PKcs-defective background reaches the level of unrepaired DSBs in Artemis-deficient cells at prolonged repair times (Riballo *et al*, 2004). Hence, we concluded that DNA-PKcs has an essential role in Artemis-dependent NHEJ, but a non-essential, facilitating role for Artemis-independent DSBs (Löbrich and Jeggo, 2005). Here we show that the level of unrepaired DSBs in DNA-PKcs-inhibited G1 cells is similar to that of Artemis-deficient G1 cells at repair times $\geqslant$24 h (Figure 7B and Supplementary Figure 7A–C). Moreover, Artemis-deficient G2 cells exhibit twice the level of unrejoined DSBs compared with Artemis-deficient G1 cells, consistent with an essential role of Artemis for the same subset of DSBs in G1 and in G2. However, DNA-PKcs-inhibited G2 cells have a much lower level of unrejoined DSBs than Artemis-deficient G2 cells at repair times $\geqslant$24 h, and show only a marginal elevation compared with WT cells (Figure 7B). Strikingly, at repair times $\geqslant$48 h, DNA-PKcs-inhibited cells display fewer unrejoined DSBs in G2 than in G1 (Figure 7B). This strongly suggests that in G2 there is no absolute requirement for DNA-PK activity for DSB repair (although NHEJ in G2 is facilitated by DNA-PKcs to the same degree as in G1) and that the essential role of Artemis in G2 for a subset of IR-induced DSBs is independent of DNA-PKcs. Taken together, our epistasis studies using DNA-PKcs inhibitors support the

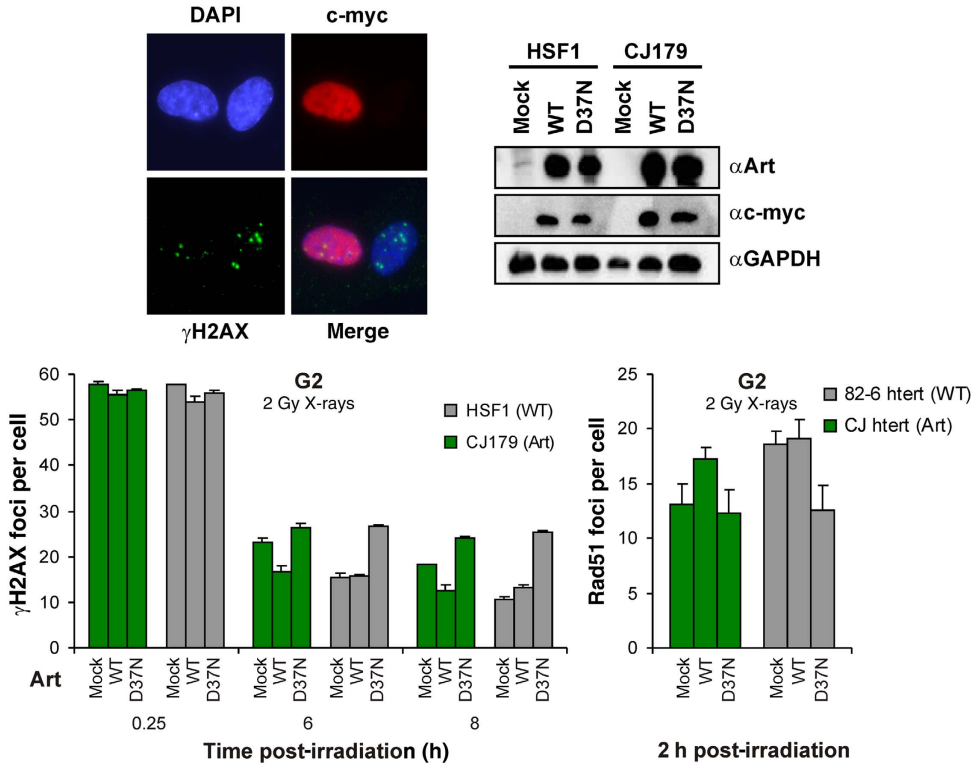

Figure 8 Artemis endonuclease activity promotes IR-induced HR in G2. The DSB-repair defect of Artemis-deficient cells (CJ179) is corrected with WT Artemis but not with an endonuclease-deficient Artemis construct (D37N), and overexpression of D37N confers a repair defect to HSF1 control cells. Analysis of γH2AX and Rad51 foci was conducted in cells positive for c-myc, that is, only cells efficiently transfected were included in the analysis. The image on the left shows two G2-phase, Artemis-deficient cells transfected with the WT Artemis construct at 8 h following 2-Gy irradiation. One of the two cells shows efficient Artemis expression (c-myc signal) and lower foci numbers. Error bars represent the s.e.m. from three different experiments. Statistical analysis revealed that Artemis-deficient cells with or without complementation of the Artemis D37N construct exhibit significantly elevated γH2AX foci levels (at 6 and 8 h) and significantly reduced Rad51 foci levels (at 2 h) compared with Artemis-deficient cells complemented with the Artemis WT construct ($P<0.05$; one-tailed Welch's test). Control cells overexpressing D37N-mutant Artemis exhibit significantly elevated γH2AX foci levels (at 6 and 8 h) and significantly reduced Rad51 foci levels (at 2 h) compared with control cells with or without overexpression of Artemis WT ($P<0.05$; one-tailed Welch's test). See Supplementary data for further information.

notion that the role of ATM and Artemis in G2 is independent of DNA-PK-dependent NHEJ.

Artemis endonuclease activity promotes DSB repair by HR

We have previously shown that Artemis endonuclease activity is important for the slow component of DSB repair by NHEJ in G1 (Riballo *et al*, 2004). Here, we analysed G2-phase, Artemis-deficient primary human fibroblasts that were efficiently transfected with Artemis expression constructs (Figure 8). Transfection with WT Artemis complemented the G2 DSB-repair defect of Artemis-deficient cells. Strikingly, transfection with the endonuclease-deficient Artemis construct (D37N) did not restore normal DSB repair (Figure 8). Furthermore, expression of WT Artemis, but not D37N Artemis, restored the Rad51 foci level of Artemis-deficient fibroblasts. We also overexpressed Artemis in control cells and observed that D37N-mutant Artemis, but not WT Artemis, increased the γH2AX foci level and decreased the Rad51 foci level (Figure 8). This provides strong evidence that Artemis promotes the early steps of HR as an endonuclease, potentially during the processing step, which is necessary to enable resection of radiation-induced DSBs.

KAP-1-dependent heterochromatin correlates with G2-phase DSB repair by HR

We recently showed that in G0/G1-phase ATM facilitates a component of NHEJ by regulating chromatin modifications in heterochromatic regions (Goodarzi *et al*, 2008). DSBs that remain unrepaired in ATM-defective or inhibited cells are enriched at densely staining DAPI chromocentres, which can be visualized in murine NIH3T3 cells. Knockdown of KAP-1, a heterochromatic building factor that is phosphorylated by ATM, relieves the requirement for ATM for DSB repair (Ziv *et al*, 2006; Goodarzi *et al*, 2008).

In our examination of G0/G1 cells, we carried out extensive analysis to verify published evidence that murine chromocentres represent heterochromatic DNA. Published, as well as our own, data suggest that this is not the case in G2 (Fischle *et al*, 2005; Goodarzi *et al*, 2009). Whereas the overall level of KAP-1 is similar in G1 and G2, the amount of KAP-1 localized to the densely staining DAPI regions is strongly reduced in G2 compared with G1 (Figure 9A and Supplementary Figure 8). Thus, the organization of chromatin is distinct in G2 phase and condensed DAPI regions represent sites of chromosome condensation prior to mitosis rather than heterochromatic chromocentres (Goodarzi *et al*, 2009). The localization of the γH2AX foci, which remain in

A

Phase	% total KAP-1 in densely staining DAPI regions	% of γ-H2AX foci that co-localise with DAPI regions at 8h	% of RPA foci that co-localise with DAPI regions at 2h
G0/G1	73	60–70	No RPA foci
Early G2	30		
Mid G2	27	33	31
Late G2	22		

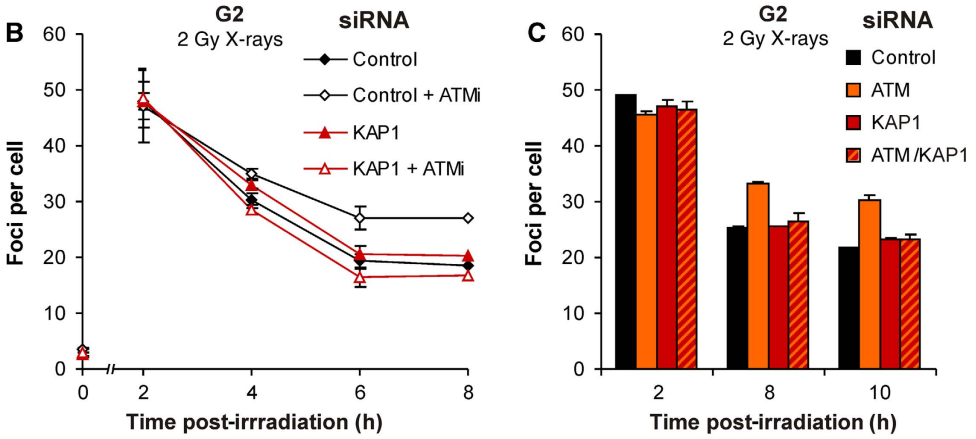

Figure 9 IR-induced HR in G2 repairs DSBs in KAP-1-associated heterochromatic DNA regions. (**A**) Quantification of % of KAP-1 in densely staining DAPI regions in G1- versus G2-phase and localization of γH2AX foci (assessed at 8 h following 2-Gy irradiation in NIH 3T3 mouse cells treated with the ATM inhibitor KU55933) and RPA foci (assessed at 2 h following 2-Gy irradiation in untreated NIH 3T3 cells). KAP-1 signal distribution was estimated by measuring the signal intensity within (i) densely staining DAPI regions and (ii) the total nuclear volume. By dividing (i) by (ii), the percentage of total KAP-1 localized to densely staining DAPI was calculated. In G2-phase, the values estimated were similar to that for the % DAPI staining, suggesting a random distribution of KAP-1, which was not the case in G1-phase where >70% of total KAP-1 was localized to densely staining DAPI, equivalent to <20% of the nuclear volume. Typical images analysed are shown in Supplementary Figure 8. The colocalization studies as well as the KAP-1 staining were performed according to Goodarzi *et al* (2008). (**B**) γH2AX foci analysis in 1BRneo cells downregulated for KAP-1 with or without the ATM inhibitor KU55933 (designated ATMi in the figure). (**C**) γH2AX foci analysis in siRNA-treated HeLa cells. Background foci numbers were subtracted from the foci numbers in the irradiated samples. Samples were evaluated in a blinded manner. Error bars represent the s.e.m. from the analysis of at least three different experiments. Statistical analysis was performed at the 8- and 10-h time points, and revealed that cells treated with control siRNA and KU55933 exhibit significantly elevated foci levels compared with cells treated with KAP-1 siRNA and KU55933. Further, cells treated with ATM siRNA exhibit significantly elevated foci levels compared with cells treated with ATM/KAP-1 double siRNA ($P<0.05$; one-tailed Welch's test). Although the repair defect is apparent and similar for the two different cell systems, the absolute foci numbers in HeLa cells are slightly higher, likely due to their higher DNA content.

the absence of ATM at 8 h post-IR, correlates with the distribution of KAP-1 in both cell-cycle phases. Although this distribution parallels the intensity of DAPI staining in G2 phase (i.e. reflects DNA distribution), the correlating change in the localization of KAP-1- and ATM-dependent γH2AX foci from G1 to G2 is marked. Further, RPA foci present at 2 h post-IR in WT cells demonstrated a localization that also correlates with KAP-1 distribution (Figure 9A and Supplementary Figure 8).

Importantly, we also examined the impact of knockdown of KAP-1 in G2 phase cells and found that it relieves the ATM-dependent DSB-repair defect in G2 as in G1 phase (Figure 9B and C), that is, DSBs, which persist in an ATM-inhibited (Figure 9B) or ATM-downregulated cell line (Figure 9C), can be repaired if KAP-1 is depleted. This strongly suggests that HR occurs at KAP-1-dependent heterochromatin regions.

Discussion

Previously, we showed that ATM and Artemis are required for a subset of DNA DSB repair that occurs with slow kinetics by NHEJ in G0/G1 phase. Here, we demonstrate that ATM and Artemis are also required for repair of a similar sized subset of DSBs, which are also rejoined with slow kinetics in G2. However, in G2 this process represents HR. Furthermore, this represents the major contribution of HR to DSB repair after IR in G2 phase, with the majority of DSBs being rejoined by NHEJ in G0/G1 and G2. These findings demonstrate that ATM and Artemis can contribute to DSB rejoining by either NHEJ or HR depending on cell-cycle phase. Previous studies have provided evidence that ATM is required for at least a component of HR (Morrison *et al*, 2000; Shrivastav *et al*, 2009), but this has not previously been shown for Artemis.

HR has its major role in dealing with replication-associated events, either by promoting repair of replication-blocking lesions or by repairing one-sided DSBs that arise at collapsed replication forks (Trenz *et al*, 2006; Hanada *et al*, 2007; Roseaulin *et al*, 2008). Since Artemis- or ATM-defective cells do not manifest the normal genomic instability and marked cross-link sensitivity of HR-defective mutants, there is no evidence that Artemis or ATM contribute to replication-associated HR events. Consistent with this, Artemis is dispensable for spontaneous SCEs. Thus, ATM and Artemis are not core HR components. However, HR also repairs two-ended DSBs in G2 and it is this situation where we uncovered a function for ATM and Artemis.

We have applied three conceptually different techniques to demonstrate the requirement of ATM and Artemis for IR-induced HR in G2. First, we used the enumeration of γH2AX foci in combination with epistasis analysis using the ATM

inhibitor KU55933 and double-siRNA approaches. This analysis showed that loss of ATM or Artemis confers a repair defect, which is similar and epistatic to that of Brca2, Rad51 and Rad54 in G2. Conclusions based on γH2AX foci analysis were confirmed by PCC analysis. Second, we developed a BrdU labelling technique to detect repair synthesis during HR in G2, and demonstrated that ATM and Artemis are required for G2 phase HR. Third, we developed and exploited a technique to quantify SCE events arising in G2-irradiated cells. Finally, the observation that ATM and Artemis are required for efficient formation of RPA, Rad51 and ssDNA foci provides further evidence for their role in promoting IR-induced HR in G2. In contrast to these results, we failed to detect any requirement for Artemis in an I-*Sce*I assay. However, this assay differs from our G2-specific assays in several ways: (i) I-*Sce*I-induced DSBs need resection for repair by HR, but do not need end processing and (ii) the I-*Sce*I assay reflects HR that arises at all cell-cycle stages including S-phase. Indeed, the fact that ATR, rather than ATM, has a larger role in this process may indicate that events in S-phase predominate where ATR, rather than ATM, may activate end resection at a DSB (Jazayeri *et al*, 2006). Our γH2AX, PCC, BrdU and RPA/Rad51 assays monitor the repair of IR-induced DSBs that arise in G2-phase, and our findings suggest that it is these HR events that require Artemis and ATM. Moreover, it is difficult to analyse specific subsets of DSBs by the I-*Sce*I method. Thus, although the I-*Sce*I approach can be informative, it has limitations and the novel pathway described here cannot be readily monitored by this assay.

Previous studies have shown that the kinetics for IR-induced DSB repair in G1 exhibit a fast and a slow component (Löbrich *et al*, 1995; Wu *et al*, 2008). The fast component removes the majority of DSBs within the first 2 h and is strongly compromised in mutants of the NHEJ pathway (Rothkamm *et al*, 2003; Kühne *et al*, 2004). The slow component in G1 represents a sub-pathway of NHEJ involving ATM and Artemis (Riballo *et al*, 2004). Previous studies by our group and others failed to observe a repair defect in HR-deficient mouse cells in G2-phase (Krüger *et al*, 2004; Wu *et al*, 2008). However, these studies used PFGE analysis, which necessitates high-radiation doses that lead to massive apoptosis in MEFs (data not shown). Here, by using low-radiation doses compatible with cell survival, we show that DSB-repair kinetics in G2 are biphasic, as in G1, and that the fast component in G2 represents NHEJ and accounts for the majority of DSB-repair events. However, the slow component of DSB repair in G2 represents HR involving Rad51, Rad54, Brca2 and, unexpectedly, ATM and Artemis. Thus, ATM and Artemis are involved in the slow component of DSB repair, which accounts for 15–20% of IR-induced DSBs in G1 and in G2. However, these DSBs are subsequently repaired by distinct repair pathways.

We recently showed that the DSBs requiring ATM for repair in G0/G1 are localized to heterochromatic DNA and that the requirement can be relieved by siRNA of KAP-1, a heterochromatic component and ATM substrate. We proposed that ATM-dependent phosphorylation of KAP-1 specifically promotes repair of DSBs located within the heterochromatin (Goodarzi *et al*, 2008). Here, we demonstrate that depleting KAP-1 relieves the ATM-dependent DSB-repair defect in G2 as in G1. This finding is supported by an analysis of the localization of RPA foci and ATM-dependent DSBs. Since KAP-1 is randomly localized in G2-phase, the random localization of RPA foci and ATM-dependent DSBs does not itself provide evidence for heterochromatic localization. However, the striking change in localization between G1- and G2-phase, which correlates with the different KAP-1 localization, is strongly supportive of the notion that HR occurs at heterochromatic DNA regions. Barlow *et al* (2008) recently reported that IR-induced DSBs are efficiently processed for HR in G1 in contrast to restriction endonuclease-induced DSBs. It has been suggested that this may result from the difference in modifying IR-induced versus endonuclease-induced DSBs prior to repair (Kanaar *et al*, 2008; Wyman *et al*, 2008). The differential response uncovered in our study reflects the processing of IR-induced heterochromatic versus euchromatic DSBs. Collectively, these findings suggest that only selective types of DSBs dependent upon their nature or localization may undergo resection, and further work is required to define the precise factors regulating whether or not resection occurs at a DSB.

Our finding that Artemis is required for efficient resection during IR-induced HR might suggest that it represents the enzyme carrying out resection. However, the observation that both spontaneous SCE levels and I-*Sce*I-induced HR do not require Artemis shows that resection can occur in the absence of Artemis. Moreover, we show that Rad51 foci formation after IR-induced HR in G2 requires CtIP, a factor, which promotes end resection during HR by interacting with the exonuclease Mre11 (Sartori *et al*, 2007; Huertas *et al*, 2008). Finally, the repair defect of Artemis-deficient cells cannot be complemented with an endonuclease-deficient Artemis construct, providing direct evidence that Artemis promotes HR as an endonuclease. An intriguing model is that Artemis is required to remove lesions or secondary structures, which arise in heterochromatic DNA regions that might otherwise inhibit resection.

We have observed here that the role of Artemis in HR is independent of DNA-PK. During NHEJ, Artemis acquires endonuclease activity following DNA-PK auto-phosphorylation at DSB termini with hairpins or single-stranded DNA overhangs (Goodarzi *et al*, 2006). Notably, we showed that phosphorylation of Artemis by DNA-PK was dispensable for nuclease activity (Goodarzi *et al*, 2006), consistent with our observation here that DNA-PK is dispensable for Artemis endonuclease activity during HR. It is possible that the proposed requirement for DNA-PK to remodel the DNA end for Artemis during NHEJ (Goodarzi *et al*, 2006) can be bypassed in some way by one or more factors during the process of HR.

Based on our findings, we suggest the following model (Figure 10): The majority of IR-induced DSBs (~80%) are repaired by NHEJ with fast kinetics in G1 and in G2, independently of ATM and Artemis. However, a subset of DSBs in G1 and G2 is repaired more slowly and requires ATM and Artemis. This slowly repairing sub-fraction of breaks is channelled into NHEJ in G1 and into HR in G2, thus requiring either the classical NHEJ or HR factors in addition to ATM and Artemis. Moreover, our finding that Artemis-deficient cells show impaired formation of ssDNA during IR-induced HR, together with the evidence that Artemis endonuclease is required for efficient DSB repair, suggests that Artemis promotes the processing step of DSB repair, which may be a prerequisite for resection of IR-induced DSBs. Finally, the observation that KAP-1 relieves the requirement for ATM for

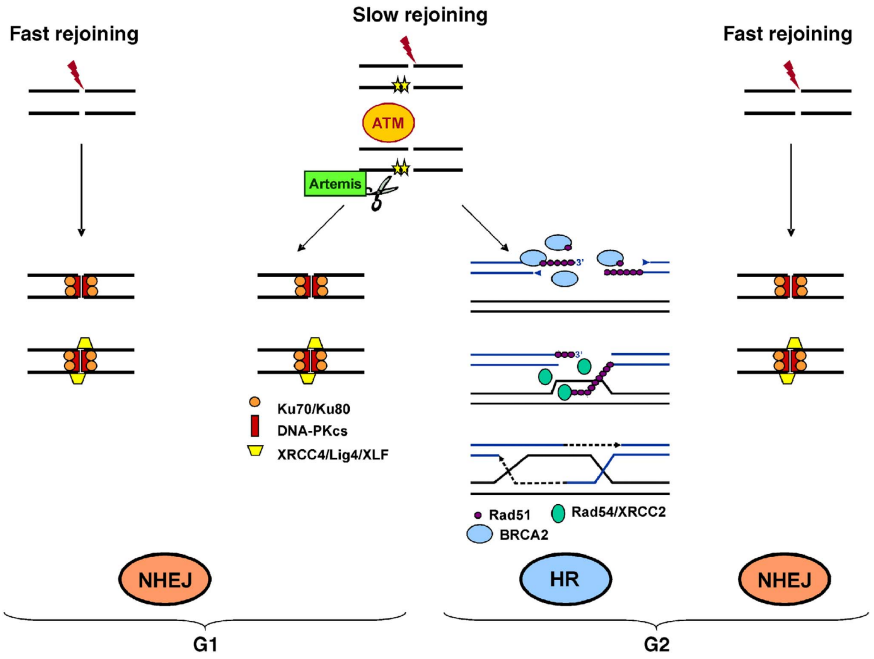

Figure 10 Pathways of DSB repair during the mammalian cell cycle (see text for explanation).

repair suggests that IR-induced HR in G2 repairs DSBs associated with heterochromatin.

Materials and methods

Cell culture

Primary human fibroblasts used were HSF1, C2906, C2886 (kindly provided by Dr M Frankenberg-Schwager) and 48BR (all derived from normal individuals), CJ179 and F01-240 (from Artemis-defective individuals), 2BN (from an XLF-deficient patient) and AT1BR (from an A-T patient). 1BRneo cells are SV40-immortalized fibroblasts from a normal individual. HSC62 are primary fibroblasts from a patient with a homozygous mutation (IVS19-1 G to A) in BRCA2 and were kindly provided by Dr M Digweed (Howlett *et al*, 2002). 82-6hTert- and CJhTert- are hTert-immortalized cell lines, derived from a normal (82-6) and an Artemis-defective cell line (CJ179), respectively. ATM$^{-/-}$, Artemis$^{-/-}$, and Lig4$^{-/-}$, MEFs were kind gifts from Drs J Chen and F Alt. Cells were cultured in minimal essential medium (MEM) or DMEM supplemented with 10% FCS and antibiotics. siRNA transfection of HeLa cells was carried out using HiPerFect Transfection Reagent (Qiagen, Hilden, Germany) following the manufacturer's instructions. siRNA transfection of 1BRneo cells was carried out using siPORTTM NeoFXTM (Ambion, Austin, TX, USA). The siRNA oligonucleotides were obtained from the Dharmacon SMARTpool. Transfection of primary human fibroblasts with WT and D37N Artemis c-Myc constructs (Goodarzi *et al*, 2006) was performed using the AMAXA transfection system (according to the manufactorer's instructions, Gaithersburg, MD). Cells positive for c-Myc (i.e. expressing the construct) were analysed for γH2AX foci. Cells pulse-labelled with 10 μM BrdU (Roche) for 1 h were analysed by FACs according to standard protocols.

Immunofluorescence

Cells grown on coverslips were fixed in 100% methanol (−20°C) for 30 min, permeabilized in acetone (−20°C) for 1 min and washed 3 × 10 min in PBS/1% FCS. Samples were incubated with primary antibodies (monoclonal or polyclonal anti-γH2AX antibody 1:200, Upstate; polyclonal anti-CENP-F antibody 1:200, Santa Cruz; polyclonal anti-phosphoH3 (pH3) antibody (Ser10) 1:200, Upstate; monoclonal anti-BrdU antibody 1:200, Becton Dickinson; polyclonal anti-RPA antibody 1:100, Calbiochem and anti -Rad51 antibody 1:100, Santa Cruz) in PBS/1% FCS for 1 h at room temperature, washed in PBS/1% FCS for 3 × 10 min and incubated with Alexa Fluor 488-, Alexa Fluor 546- or Alexa Fluor 594-conjugated secondary antibodies (MoBiTec, 1:500) for 1 h at room temperature. Cells were washed in PBS for 4 × 10 min and mounted using Vectashield mounting medium containing 4,6-diamidino-2-phenylindole (DAPI; Vector Laboratories, Burlingame, CA). In a single experiment, cell counting was performed until at least 40 cells and 40 foci were registered per sample. For data points that were derived from a single experiment, the error bars represent the s.e.m. from the analysis of all cells. For data points that were derived from more than one experiment, the error bars represents the s.e.m. between the independent experiments, which is typically higher than the s.e.m. from all analysed cells. Statistical analysis using the Student's t-test was performed at critical time points to evaluate the significance of differences in foci levels.

PCC and SCE analysis, chemicals and irradiation

For PCC analysis, cells were treated with 50 ng/ml calyculin A (Calbiochem) for 30 min before harvesting. For SCE analysis, cells were grown for 48 h in BrdU before irradiation. Colcemid (together with 1 mM caffeine to overcome the G2/M arrest) was added at 8 h until 12 h post-irradiation to collect cells in mitosis. Chromatid breaks (for PCC analysis) or SCEs were scored in at least 100 chromosome spreads from at least three independent experiments per data point. Staining was according to standard protocols. Aphidicolin (Sigma) was added at 1 μg/ml immediately before IR. ATM inhibitor (KU55933) and DNA-PK inhibitor (NU7026), a kind gift from Kudos Pharmaceuticals (Cambridge, UK), were added at 20 μM 60 min prior to IR. X-ray irradiation was performed at 90- or 120-kV γ-irradiation using a ^{137}Cs source. Dosimetry was performed with ion chambers and considered the increase in dose for cells grown on glass coverslips relative to plastic surfaces (Kegel *et al*, 2007).

Supplementary data

Supplementary data are available at *The EMBO Journal* Online (http://www.embojournal.org).

Acknowledgements

We thank Dr G Smith for providing the ATM inhibitor KU55933. The ML laboratory is supported by the Deutsche Forschungsgemeinschaft (Grant LO 677/4-1/2), the Bundesministerium für Bildung und Forschung via the Forschungszentrum Karlsruhe (Grants 02S8135 and 02S8355) and the Wilhelm Sander-Stiftung (2003.114.1/3). The PAJ laboratory is supported by the Medical Research Council, the Association for International Cancer

Research, the Leukaemia Research Fund, the Department of Health and EU grant (FIGH-CT-200200207) (DNA repair). Both laboratories are supported by EU Grant FI6R-CT-2003-508842 (RiscRad).

Conflict of interest

The authors declare that they have no conflict of interest.

References

Ahnesorg P, Smith P, Jackson SP (2006) XLF interacts with the XRCC4–DNA ligase IV complex to promote DNA nonhomologous end-joining. *Cell* **124:** 301–313

Allen C, Kurimasa A, Brenneman MA, Chen DJ, Nickoloff JA (2002) DNA-dependent protein kinase suppresses double-strand break-induced and spontaneous homologous recombination. *Proc Natl Acad Sci USA* **99:** 3758–3763

Asakawa Y, Gotoh E (1997) A method for detecting sister chromatid exchanges using prematurely condensed chromosomes and immunogold–silver staining. *Mutagenesis* **12:** 175–177

Barlow JH, Lisby M, Rothstein R (2008) Differential regulation of the cellular response to DNA double-strand breaks in G1. *Mol Cell* **30:** 73–85

Bekker-Jensen S, Lukas C, Kitagawa R, Melander F, Kastan MB, Bartek J, Lukas J (2006) Spatial organization of the mammalian genome surveillance machinery in response to DNA strand breaks. *J Cell Biol* **173:** 195–206

Buck D, Malivert L, de Chasseval R, Barraud A, Fondanèche MC, Sanal O, Plebani A, Stéphan JL, Hufnagel M, le Deist F, Fischer A, Durandy A, de Villartay JP, Revy P (2006) Cernunnos, a novel nonhomologous end-joining factor, is mutated in human immunodeficiency with microcephaly. *Cell* **124:** 287–299

Darroudi F, Wiegant W, Meijers M, Friedl AA, van der Burg M, Fomina J, van Dongen JJ, van Gent DC, Zdzienicka MZ (2007) Role of Artemis in DSB repair and guarding chromosomal stability following exposure to ionizing radiation at different stages of cell cycle. *Mutat Res* **615:** 111–124

Deckbar D, Birraux J, Krempler A, Tchouandong L, Beucher A, Walker S, Stiff T, Jeggo PA, Löbrich M (2007) Chromosome breakage after G2 checkpoint release. *J Cell Biol* **176:** 749–755

Esashi F, Galkin VE, Yu X, Egelman EH, West SC (2007) Stabilization of RAD51 nucleoprotein filaments by the C-terminal region of BRCA2. *Nat Struct Mol Biol* **14:** 468–474

Fischle W, Tseng BS, Dormann HL, Ueberheide BM, Garcia BA, Shabanowitz J, Hunt DF, Funabiki H, Allis CD (2005) Regulation of HP1–chromatin binding by histone H3 methylation and phosphorylation. *Nature* **438:** 1116–1122

Goodarzi AA, Noon AT, Deckbar D, Ziv Y, Shiloh Y, Löbrich M, Jeggo PA (2008) ATM signaling facilitates repair of DNA double-strand breaks associated with heterochromatin. *Mol Cell* **31:** 167–177

Goodarzi AA, Noon AT, Jeggo PA (2009) The impact of heterochromatin on DSB repair. *Biochem Soc Trans* **37:** 569–576

Goodarzi AA, Yu Y, Riballo E, Douglas P, Walker SA, Ye R, Härer C, Marchetti C, Morrice N, Jeggo PA, Lees-Miller SP (2006) DNA-PK autophosphorylation facilitates Artemis endonuclease activity. *EMBO J* **25:** 3880–3889

Hanada K, Budzowska M, Davies SL, van Drunen E, Onizawa H, Beverloo HB, Maas A, Essers J, Hickson ID, Kanaar R (2007) The structure-specific endonuclease Mus81 contributes to replication restart by generating double-strand DNA breaks. *Nat Struct Mol Biol* **14:** 1096–1104

Hinz JM, Yamada NA, Salazar EP, Tebbs RS, Thompson LH (2005) Influence of double-strand-break repair pathways on radiosensitivity throughout the cell cycle in CHO cells. *DNA Rep (Amst)* **4:** 782–792

Howlett NG, Taniguchi T, Olson S, Cox B, Waisfisz Q, De Die-Smulders C, Persky N, Grompe M, Joenje H, Pals G, Ikeda H, Fox EA, D'Andrea AD (2002) Biallelic inactivation of BRCA2 in Fanconi anemia. *Science* **297:** 606–609

Huertas P, Cortés-Ledesma F, Sartori AA, Aguilera A, Jackson SP (2008) CDK targets Sae2 to control DNA-end resection and homologous recombination. *Nature* **455:** 689–692

Jazayeri A, Falck J, Lukas C, Bartek J, Smith GC, Lukas J, Jackson SP (2006) ATM- and cell cycle-dependent regulation of ATR in response to DNA double-strand breaks. *Nat Cell Biol* **8:** 37–45

Johnson RD, Jasin M (2000) Sister chromatid gene conversion is a prominent double-strand break repair pathway in mammalian cells. *EMBO J* **19:** 3398–3407

Kao GD, McKenna WG, Yen TJ (2001) Detection of repair activity during the DNA damage-induced G2 delay in human cancer cells. *Oncogene* **20:** 3486–3496

Kanaar R, Wyman C, Rothstein R (2008) Quality control of DNA break metabolism: in the 'end', it's a good thing. *EMBO J* **27:** 581–588

Kegel P, Riballo E, Kühne M, Jeggo PA, Löbrich M (2007) X-irradiation of cells on glass slides has a dose doubling impact. *DNA Repair (Amst)* **6:** 1692–1697

Krüger I, Rothkamm K, Löbrich M (2004) Enhanced fidelity for rejoining radiation-induced DNA double-strand breaks in the G2 phase of Chinese Hamster Ovary cells. *Nucleic Acids Res* **32:** 2677–2684

Kühne M, Riballo E, Rief N, Rothkamm K, Jeggo PA, Löbrich M (2004) A double-strand break repair defect in ATM-deficient cells contributes to radiosensitivity. *Cancer Res* **64:** 500–508

Li Y, Chirgadze DY, Bolanos-Garcia VM, Sibanda BL, Davies OR, Ahnesorg P, Jackson SP, Blundell TL (2008) Crystal structure of human XLF/Cernunnos reveals unexpected differences from XRCC4 with implications for NHEJ. *EMBO J* **27:** 290–300

Liang F, Romanienko PJ, Weaver DT, Jeggo PA, Jasin M (1996) Chromosomal double-strand break repair in Ku80-deficient cells. *Proc Natl Acad Sci USA* **93:** 8929–8933

Liao H, Winkfein RJ, Mack G, Rattner JB, Yen TJ (1995) CENP-F is a protein of the nuclear matrix that assembles onto kinetochores at late G2 and is rapidly degraded after mitosis. *J Cell Biol* **130:** 507–518

Lieber MR (2008) The mechanism of human nonhomologous DNA end joining. *J Biol Chem* **283:** 1–5

Löbrich M, Rydberg B, Cooper PK (1995) Repair of X-ray-induced DNA double-strand breaks in specific *Not*I restriction fragments in human fibroblasts: joining of correct and incorrect ends. *Proc Natl Acad Sci USA* **92:** 12050–12054

Löbrich M, Jeggo PA (2005) Harmonising the response to DSBs: a new string in the ATM bow. *DNA Rep (Amst)* **4:** 749–759

Löbrich M, Jeggo PA (2007) The impact of a negligent G2/M checkpoint on genomic instability and cancer induction. *Nat Rev Cancer* **7:** 861–869

Miyazaki T, Bressan DA, Shinohara M, Haber JE, Shinohara A (2004) *In vivo* assembly and disassembly of Rad51 and Rad52 complexes during double-strand break repair. *EMBO J* **25:** 939–949

Morrison C, Sonoda E, Takao N, Shinohara A, Yamamoto K, Takeda S (2000) The controlling role of ATM in homologous recombinational repair of DNA damage. *EMBO J* **19:** 463–471

Moynahan ME, Chiu JW, Koller BH, Jasin M (1999) Brca1 controls homology-directed DNA repair. *Mol Cell* **4:** 511–518

Moynahan ME, Pierce AJ, Jasin M (2001) BRCA2 is required for homology-directed repair of chromosomal breaks. *Mol Cell* **7:** 263–272

Nussenzweig A, Nussenzweig MC (2007) A backup DNA repair pathway moves to the forefront. *Cell* **131:** 223–225

Pannicke U, Ma Y, Hopfner KP, Niewolik D, Lieber MR, Schwarz K (2004) Functional and biochemical dissection of the structure-specific nuclease ARTEMIS. *EMBO J* **23:** 1987–1997

Pierce AJ, Johnson RD, Thompson LH, Jasin M (1999) XRCC3 promotes homology-directed repair of DNA damage in mammalian cells. *Genes Dev* **13:** 2633–2638

Riballo E, Kühne M, Rief N, Doherty A, Smith GC, Recio MJ, Reis C, Dahm K, Fricke A, Krempler A, Parker AR, Jackson SP, Gennery A, Jeggo PA, Löbrich M (2004) A pathway of double-strand break rejoining dependent upon ATM, Artemis, and proteins locating to γH2AX foci. *Mol Cell* **16:** 715–724

Roseaulin L, Yamada Y, Tsutsui Y, Russell P, Iwasaki H, Arcangioli B (2008) Mus81 is essential for sister chromatid recombination at broken replication forks. *EMBO J* **27:** 1378–1387

Rothkamm K, Krüger I, Thompson LH, Löbrich M (2003) Pathways of DNA double-strand break repair during the mammalian cell cycle. *Mol Cell Biol* **23:** 5706–5715

Sartori AA, Lukas C, Coates J, Mistrik M, Fu S, Bartek J, Baer R, Lukas J, Jackson SP (2007) Human CtIP promotes DNA end resection. *Nature* **22:** 509–514

Shrivastav M, Miller CA, De Haro LP, Durant ST, Chen BP, Chen DJ, Nickoloff JA (2009) DNA-PKcs and ATM co-regulate DNA double-strand break repair. *DNA Repair (Amst)* **8:** 920–929

Sonoda E, Sasaki MS, Morrison C, Yamaguchi-Iwai Y, Takata M, Takeda S (1999) Sister chromatid exchanges are mediated by homologous recombination in vertebrate cells. *Mol Cell Biol* **19:** 5166–5169

Soulas-Sprauel P, Rivera-Munoz P, Malivert L, Le Guyader G, Abramowski V, Revy P, Villartay JP (2007) V(D)J and immunoglobulin class switch recombinations: a paradigm to study the regulation of DNA end-joining. *Oncogene* **26:** 7780–7791

Taghian DG, Nickoloff JA (1997) Chromosomal double-strand breaks induce gene conversion at high frequency in mammalian cells. *Mol Cell Biol* **17:** 6386–6393

Thompson LH, Schild D (2002) Recombinational DNA repair and human disease. *Mutat Res* **509:** 49–78

Thorslund T, West SC (2007) BRCA2: a universal recombinase regulator. *Oncogene* **26:** 7720–7730

Trenz K, Smith E, Smith S, Costanzo V (2006) ATM and ATR promote Mre11 dependent restart of collapsed replication forks and prevent accumulation of DNA breaks. ATM and ATR promote Mre11 dependent restart of collapsed replication forks and prevent accumulation of DNA breaks. *EMBO J* **25:** 1764–1774

van der Burg M, Verkaik NS, den Dekker AT, Barendregt BH, Pico-Knijnenburg I, Tezcan I, vanDongen JJ, van Gent DC (2007) Defective Artemis nuclease is characterized by coding joints with microhomology in long palindromic-nucleotide stretches. *Eur J Immunol* **37:** 3522–3528

van Gent DC, van der Burg M (2007) Non-homologous end-joining, a sticky affair. *Oncogene* **26:** 7731–7740

Wang H, Wang H, Powell SN, Iliakis G, Wang Y (2004) ATR affecting cell radiosensitivity is dependent on homologous recombination repair but independent of nonhomologous end joining. *Cancer Res* **64:** 7139–7143

Wang J, Pluth JM, Cooper PK, Cowan MJ, Chen DJ, Yannone SM (2005) Artemis deficiency confers a DNA double-strand break repair defect and Artemis phosphorylation status is altered by DNA damage and cell cycle progression. *DNA Repair (Amst)* **4:** 556–570

West SC (2003) Molecular views of recombination proteins and their control. *Nat Rev Mol Cell Biol* **4:** 435–445

Weterings E, Chen DJ (2008) The endless tale of non-homologous end-joining. *Cell Res* **18:** 114–124

Wu W, Wang M, Wu W, Singh SK, Mussfeldt T, Iliakis G (2008) Repair of radiation induced DNA double strand breaks by backup NHEJ is enhanced in G2. *DNA Repair (Amst)* **7:** 329–338

Wyman C, Kanaar R (2006) DNA double-strand break repair: all's well that ends well. *Annu Rev Genet* **40:** 363–383

Wyman C, Warmerdam DO, Kanaar R (2008) From DNA end chemistry to cell-cycle response: the importance of structure, even when it's broken. *Mol Cell* **30:** 5–6

Yuan SS, Chang HL, Lee EY (2003) Ionizing radiation-induced Rad51 nuclear focus formation is cell cycle-regulated and defective in both ATM(−/−) and c-Abl(−/−) cells. *Mutat Res* **525:** 85–92

Yuan SS, Lee SY, Chen G, Song M, Tomlinson GE, Lee EY (1999) BRCA2 is required for ionizing radiation-induced assembly of Rad51 complex *in vivo*. *Cancer Res* **59:** 3547–3551

Ziv Y, Bielopolski D, Galanty Y, Lukas C, Taya Y, Schultz DC, Lukas J, Bekker-Jensen S, Bartek J, Shiloh Y (2006) Chromatin relaxation in response to DNA double-strand breaks is modulated by a novel ATM- and KAP-1 dependent pathway. *Nat Cell Biol* **8:** 870–876